Substantial stabilization of ferromagnetism in ZnO:Mn induced by N codoping

2009 J. Phys.: Condens. Matter 21 185503

(http://iopscience.iop.org/0953-8984/21/18/185503)

J. Phys.: Condens. Matter **21** (2009) 185503 (4pp) doi:10.1088/0953-8984/21/18/185503

Substantial stabilization of ferromagnetism in ZnO:Mn induced by N codoping

M H N Assadi, Y B Zhang and S Li

School of Materials Science and Engineering, University of New South Wales, Sydney, New South Wales 2052, Australia

E-mail: y.zhang@unsw.edu.au

Received 22 January 2009, in final form 6 March 2009
Published 31 March 2009
Online at stacks.iop.org/JPhysCM/21/185503

Abstract

Electronic structures and magnetic properties of ZnO:Mn and ZnO:Mn + N systems are investigated using first-principles density functional calculations with generalized gradient approximation. The results provide a fundamental theoretical understanding in the substantial ferromagnetic stability induced by N codoping in the ZnO:Mn system observed experimentally. They demonstrate that the ferromagnetic interaction is due to the hybridization between N 2p and Mn 3d states and is very sensitive to the geometrical configurations of dopants in the ZnO host lattice. The most stable ferromagnetic configuration corresponds to the Mn–N–Mn cluster, energetically strong enough to lead to hole-mediated ferromagnetism at room temperature.

(Some figures in this article are in colour only in the electronic version)

Diluted magnetic semiconductors (DMS) have attracted scientific interest because of their unique spintronic properties with possible technological applications [1, 2]. Room temperature ferromagnetism was theoretically predicted to appear in heavily p-type doped ZnO [3]. It made the ZnO:Mn system one of the most studied DMS for applications requiring ferromagnetism near room temperature. Subsequently some theoretical [4–6] and experimental [7] work showed that ZnO:Mn possesses no room temperature ferromagnetism. It was believed that the weak ferromagnetism appearing at room temperature in bulk and transparent thin films of Mn-doped ZnO [8] was associated with phase-segregated impurities such as Zn-doped Mn_2O_3 [9] or Mn_3O_4 [10]. However, further experimental results demonstrated that ferromagnetism could be induced by introducing free carriers in the system through the codoping technique. First-principles density functional calculations suggested that N was one of the best candidates to be used to introduce p-type ZnO:Mn DMS [4, 5]. ZnO doped with at least 10% of Mn and a similar amount of N was predicted to have a ferromagnetic ground state stabilized by 10 meV per primitive cell. The investigation into the possible realization of room temperature ferromagnetic N-codoped ZnO:Mn $(10\bar{1}0)$ thin films proposed that N codoping would enhance the stability of a ferromagnetic state over an antiferromagnetic state [11]. A clear correlation between N and high Curie temperature ferromagnetism was demonstrated in ZnO:Mn nanocrystalline films [12]. Recently the N-doped $Zn_{0.95}Mn_{0.05}O$ film showed a ferromagnetic ordering below 80 K while the undoped films showed a paramagnetic behavior at all temperatures investigated [13]. However, magnetic interaction mechanisms and their possible geometry configurations of dopants are still unclear. In this work, the effect of N codoping on electronic spin alignment of Mn-doped ZnO is systematically investigated using first-principles calculations and the preference of N sites is revealed.

Band structure and total energy calculations using first-principles density functional theory (DFT) were performed using the CASTEP program [14] with the plane wave pseudopotential approach. Generalized gradient approximation (GGA) [15] was employed to simulate the electron's exchange–correlation energy. The energy cutoff was 800 eV and a k mesh of $3 \times 3 \times 1$ was used for integration over the Brillouin zone of a 32-atom ZnO host supercell ($2a \times 2a \times 2c$) as these calculation settings are proven to give accurate results for magnetic systems [16]. ZnO:Mn lattice parameters were fixed to experimental values of $a = 3.26$, $c = 5.22$ and $u = 0.425$ for an Mn doping level of 12.5% [17]. Internal coordinates of all atoms were allowed to relax through the use of

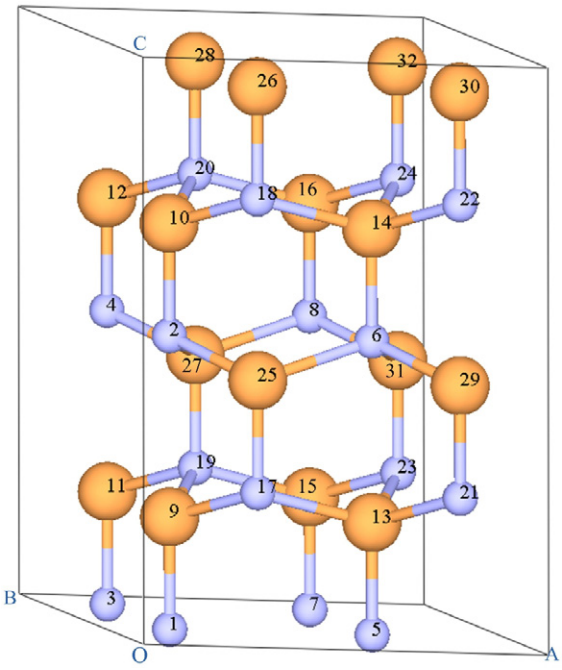

Figure 1. A 32-atom $2 \times 2 \times 2$ ZnO supercell. The large and small balls indicate O and Zn lattice sites, respectively.

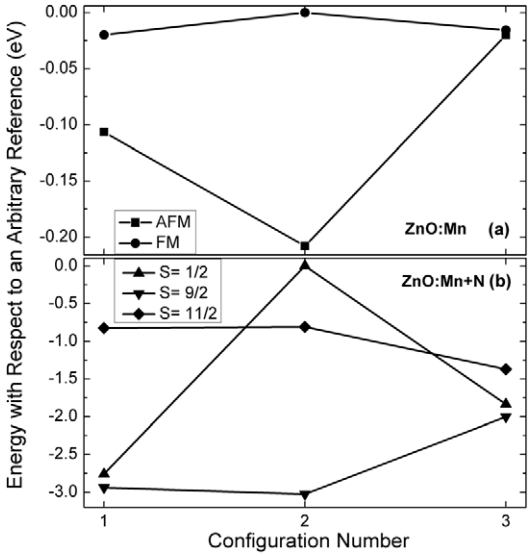

Figure 2. Total energies for the three configurations in (a) the ZnO:Mn system for both ferromagnetic (FM) and antiferromagnetic (AFM) Mn spin alignment and (b) the ZnO:Mn + N system for spin $1/2$, $9/2$ and $11/2$ alignment. In both systems energies were calculated with respect to an arbitrary energy origin, making the comparison tractable.

Hellmann–Feynman forces while the spin of every individual atom was fixed to its initial formal state. The density mixing scheme [18] was used for self-consistent electronic minimization that complies with spin restrictions.

Firstly the effect of Mn doping in the ZnO host without any additional carrier doping was examined. Since two Mn's are essential for the study of spin alignment, two Zn^{2+} ions were chosen to be substituted with Mn^{2+} ions in the 32-atom ZnO supercell shown in figure 1. As a result the chemical formula of our supercell is $Zn_{14}Mn_2O_{16}$, which is equivalent to an Mn concentration of 12.5% ($Zn_{0.875}Mn_{0.125}O$). The two Mn ions can be either isolated or paired to be a dimer intermediated by an oxygen. Thus the total energy in three typical geometrical configurations was calculated. Mn (sites 17 and 6) ions were paired along the c direction intermediated by one O (site 25) with the closest distance of 3.22 Å in configuration 1, or Mn (sites 17 and 19) ions within the ab plane intermediated by one O (site 9) with a distance of 3.26 Å in configuration 2 while they (sites 17 and 24) were isolated with the furthest distance of 6.15 Å in configuration 3. With these configurations we can investigate the behavior of paired and isolated Mn dopant ions in the ZnO host. To study the effect of possible carrier doping, the system was subsequently doped with one nitrogen ion to substitute one oxygen ion. Thus the chemical formula of our supercell becomes $Zn_{14}Mn_2O_{15}N_1$ ($Zn_{0.875}Mn_{0.125}O_{0.9375}N_{0.0625}$). Among many configuration possibilities the nitrogen ion was placed somewhere between the Mn ions [16]. It makes (1) the Mn ions were paired by one nitrogen (site 25 and 9 in the first and second configurations, respectively) and (2) one nitrogen (site 29) was located far from the two isolated Mn ions in the third configuration. The doped N ion with a formal charge of $-2e$ leaves an unpaired electron which would contribute to the total spin of the system. Therefore, three different spin states can be identified in the ZnO:Mn + N system. Firstly Mn ions possess parallel spins with the N spin parallel to them, leading to a formal spin number of $11/2$; secondly Mn ions with the N spin antiparallel to them resulting in a formal spin number of $9/2$, and finally the Mn spins are antiparallel to each other with the N parallel to one of them, that is, a formal spin number of $1/2$. Figure 2 presents the total energy calculated for (a) the ZnO:Mn system for both ferromagnetic (FM) and antiferromagnetic (AFM) Mn spin alignment and (b) the ZnO:Mn + N system for spin $1/2$, $9/2$ and $11/2$ alignment. Figure 2(a) shows that the ZnO:Mn system possesses no FM behavior as the AFM state is more stable than the FM state for all configurations. ΔE, the difference between AFM and FM states per Mn ion, was found to be -43, -104 and -8 meV for the first, second and third configurations, respectively, indicating that in the ZnO:Mn system the Mn ions do not couple ferromagnetically with each other. It can be observed that, as the Mn ions change from being paired to being isolated, ΔE decreases sharply and approaches zero, signifying a lack of spin coupling and thus a paramagnetic behavior for isolated Mn ions. The total energy of the AFM state for configurations 1 and 2 was found to be significantly lower than that for configuration 3, indicating a clustering tendency among Mn dopant ions. Furthermore the total energy of the AFM state for configuration 2 is smaller by 101 meV than that for configuration 1 and by 188 meV than that for configuration 3, suggesting the energetically preferred clustering along the ab plane. Figure 2(b) shows a radically different story for N codoping. Here the spin $9/2$ state is far more stable for all three configurations, demonstrating that the Mn ions are ferromagnetically coupled, polarizing the spin of the intermediated N anion antiferromagnetically. For configurations 1 and 3, the spin $9/2$ state is more stable by

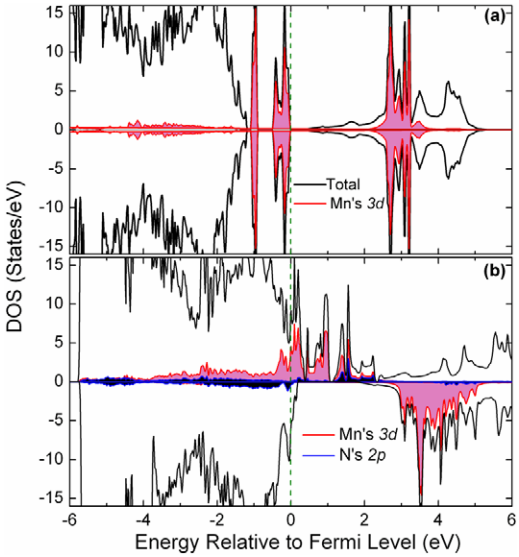

Figure 3. Total and partial density of states of (a) the ZnO:Mn system and (b) the ZnO:Mn + N system. Bold black lines stand for the total DOS while the red (blue) shaded area represents the Mn 3d (N 2p) partial DOS.

180 and 166 meV, respectively, over the spin 1/2 (AFM) state, suggesting that the presence of N dopants establishes a parallel coupling between Mn's magnetic moments via an antiparallel N. It is interesting to note that substantial stabilization occurs when Mn ions are paired along the *ab* plane in configuration 2. The spin 9/2 state is more stable by 2.20 and 3.02 eV than the spin 11/2 and spin 1/2 states, respectively. These results indicate that FM coupling is mostly stabilized for configuration 2 which can result in room temperature ferromagnetism without any doubt. Additionally the clustering tendency is a more vividly observable effect upon N doping since the total energy of the spin 9/2 state for configurations 1 and 2 is lower by approximately 1.00 eV than that for configuration 3.

To reveal the mechanism behind the change of magnetic behavior induced by N codoping, the density of state (DOS) and spatial charge and spin density for the most stable configuration of both ZnO:Mn and ZnO:Mn + N systems were analyzed where neighboring Mn ions are paired within the *ab* plane. The total DOS and Mn 3d partial DOS of the ZnO:Mn system are presented in figure 3(a). It can be seen that the occupied Mn 3d states have been split into a lower doublet (e_g) and a higher triplet (t_{2g}) due to the crystal field. All these states are lying in the valence band while the unoccupied states are far away in the conduction band. Consequently doped Mn ions provide the semiconductor with no free carriers. This means that any carrier-induced ferromagnetism cannot be achieved in the ZnO:Mn. Additionally spin-up and spin-down states are degenerate, indicating the absence of ferromagnetic exchange via O 2p electrons. Figure 3(b) presents the total DOS and partial Mn 3d and N 2p DOS of the ZnO:Mn + N system. The Fermi level is found not to be in a DOS vanishing region any more. The majority of states near and above the Fermi level belong to the upward polarized Mn 3d electrons. Moreover there is a strong hybridization between Mn 3d and N 2p with some overlapped peaks near and above the Fermi level.

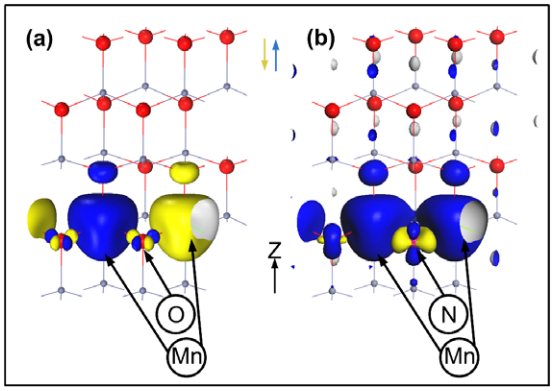

Figure 4. Spin density (a) due to Mn ions in the second configuration of the ZnO:Mn system with antiferromagnetic alignment and (b) due to Mn and N ions in the second configuration of the ZnO:Mn + N system with the spin 9/2 state. Iso-surfaces cover all points of the charge density of $0.025e$ Å^{-3}.

Therefore it can be concluded that N codoping will lead to both stabilization of ferromagnetism and introducing carriers, thus making the ZnO:Mn + N system an intrinsic dilute magnetic semiconductor.

Figure 4 shows the spin distribution for the most stable configuration of both systems. Figure 4(a) presents the spin density of the AFM state for the second configuration of the ZnO:Mn system. The bond angle of the Mn–O–Mn is calculated to be 107°46′, favoring the antiferromagnetic kinetic superexchange via the intermediating oxygen as the spin charge density demonstrates. Furthermore each Mn ion magnetizes only four oxygen ions in its coordination, indicating that no long-range indirect exchange interaction exists among Mn ions when they are separated by more than one O. This explains the aforementioned paramagnetic behavior of separated Mn ions. Figure 4(b) shows the spin density of the spin 9/2 state for the second configuration of the ZnO:Mn + N system. The bond angle of the Mn–N–Mn is 108°29′, favoring ferromagnetic superexchange via a N^{2-} ion. It is also believed that the spin 9/2 alignment will save kinetic energy by increasing the probability of electron hopping from Mn^{2+} t_{2g} orbitals to N^{2-} $2p_z$ empty orbital without changing spin direction. Our calculation shows that, in this configuration there is an extra magnetic moment of 0.24 μ_B distributed among O ions within the supercell, which can be observed in figure 4(b).

In summary, the mechanism behind the paramagnetic behavior of ZnO:Mn has been demonstrated by first-principles density functional calculations. Nitrogen codoping has been found to lead to a transition from paramagnetism to ferromagnetism. The ferromagnetic interaction in the ZnO:Mn + N system is carrier-mediated. Results also show that the ferromagnetism strongly depends on the geometrical configurations of the dopant ions, Mn and N. Clustering tendency among dopant ions exists in both systems.

Acknowledgments

This work was supported by the Australia Research Council (DP0770424 and DP0665539).

References

[1] Ohno H 1998 *Science* **281** 951
[2] Furdyna J K 1988 *J. Appl. Phys.* **64** R29
[3] Dietl T, Ohno H, Matsukura F, Cibert J and Ferrand D 2000 *Science* **287** 1019
[4] Sato K and Katayama-Yoshida H 2000 *Japan. J. Appl. Phys.* **39** L555
[5] Sato K and Katayama-Yoshida H 2001 *Japan. J. Appl. Phys.* **40** L334
[6] Feng X 2004 *J. Phys.: Condens. Matter* **16** 4251
[7] Lawes G, Risbud A S, Ramirez A P and Seshadri R 2005 *Phys. Rev.* B **71** 045201
[8] Sharma P, Gupta A, Rao K V, Owens F J, Sharma R, Ahuja R, Osorio Guillen J M, Johansson B and Gehring G A 2003 *Nat. Mater.* **2** 673
[9] Kundaliya D C, Ogale S B, Loftland S E, Dhar S, Metting C J, Shinde S R, Ma Z, Varughese B, Ramanujachary K V, Salamanca-Riba L and Venkatesan T 2004 *Nat. Mater.* **3** 709
[10] Zheng R K, Liu H, Zhang X X, Roy V A L and Djurisic A B 2004 *Appl. Phys. Lett.* **85** 2589
[11] Wang Q, Sun Q, Jena P and Kawazoe Y 2004 *Phys. Rev.* B **70** 052408
[12] Kittilstved K R, Norberg N S and Gamelin D R 2005 *Phys. Rev. Lett.* **94** 147209
[13] Yuldashev S U, Igamberdiev K T, Kang T W, Pelenovich V O and Shashkov A G 2008 *Appl. Phys. Lett.* **93** 092503
[14] Segall M D, Lindan P J D, Probert M J, Pickard C J, Hasnip P J, Clark S J and Payne M C 2002 *J. Phys.: Condens. Matter* **14** 2717
[15] Perdew J P, Chevary J A, Vosko S H, Jackson K A, Pederson M R, Singh D J and Fiolhais C 1992 *Phys. Rev.* B **46** 6671
[16] Assadi M H N, Zhang Y B and Li S 2009 *J. Appl. Phys.* **105** 043906
[17] Kolesnik S, Dabrowski B and Mais J 2004 *J. Appl. Phys.* **95** 2582
[18] Kresse G and Furthmüller J 1996 *Phys. Rev.* B **54** 11169